Journal of Guidance, Control, and Dynamics
Vol. 34, No. 1, January–February 2011

Engineering Notes

Stability Limits of Spinning Missiles with Attitude Autopilot

Xiaoyong Yan,* Shuxing Yang,† and Fenfen Xiong‡
Beijing Institute of Technology,
100081 Beijing, People's Republic of China

DOI: 10.2514/1.51627

Nomenclature

A	=	$I_P\dot{\gamma}/qSL$
C	=	I_Q/qSL
C_{ma}	=	magnus moment derivative coefficient, $\mathrm{s/rad^2}$
C_r	=	control moment derivative coefficient, 1/rad
C_δ	=	static moment derivative coefficient, 1/rad
$C_{\dot{\delta}}$	=	damping moment derivative coefficient, s/rad
I_P, I_Q	=	roll and lateral moment of inertia, $\mathrm{kg \cdot m^2}$
k_r	=	dynamic gain of servo system
k_s	=	gain of servo system
k_ω	=	gain of rate feedback
k_z	=	gain of attitude feedback
L	=	reference length, m
n_{cy}, n_{cz}	=	control command along Oy_4 and Oz_4
$Ox_5y_5z_5$	=	nonspinning velocity coordinate
q	=	dynamic pressure, $\mathrm{N/m^2}$
S	=	reference area, $\mathrm{m^2}$
T_s	=	reciprocal of natural frequency of servo system, s
γ	=	roll angle, rad
γ_c	=	coupling angle of the servo system, rad
γ_d	=	total delay angle of the system, rad
γ_l	=	lead angle of the command, rad
γ_m	=	roll angle measured by feedback element, rad
δ	=	nutation angle, rad
δ_2, δ_1	=	nutation angle on plane Ox_5y_5 and plane Ox_5z_5, rad
ϑ	=	pitch angle, rad
μ_s	=	damping ratio of servo system
σ_{cz}, σ_{cy}	=	command of servo in nonspinning body coordinate, rad
σ_1, σ_2	=	control surface angle in nonspinning body coordinate, rad
τ	=	time delay of control system, s
ψ	=	yaw angle, rad

I. Introduction

As ONE of the typical autopilots, the attitude autopilot can stabilize static unstable airframes, improve control responses, and maintain constant flight parameters. This type of autopilot has been widely applied in missiles attacking static or low-speed targets. The stability and design of the attitude autopilot have been discussed extensively for nonspinning missiles. However, for spinning missiles, this autopilot may be dynamically unstable in the form of a divergent conning motion due to the existence of cross-coupling effects. Therefore, the stability boundary of an autopilot applicable to a nonspinning missile is no longer valid in the event of spinning. This problem has been indicated in our previous paper on the stability boundary of the coning motion for spinning missiles with damping loops [1]. In this paper, we focus on the quantitative description of the stability limits associated with the attitude autopilot for spinning missiles.

Previous researches on the stability of coning motion for spinning missiles have mainly focused on uncontrolled missiles [2–4], while most recently, spinning missiles with attitude autopilots have been actively discussed. Mracek et al. have pointed out that spinning affects not only the response but also the stability of the autopilot [5]. A set of mathematical models of spinning missiles and the corresponding autopilots were established by Zipfel [6]. The design and simulation of the attitude control for spinning missiles with separated pitch and yaw control were implemented by Creagh and Mee [7]. The active control on nutation and procession motions for exospheric spinning missiles via an attitude control system was studied by Elias [8]. Adopting the linear control theory, the analysis and design of an autopilot for a spinning missile were conducted by Lestage [9]. Garnell noticed the existence of an additional phase lag of servo at the missile spinning frequency, and analyzed the variation of the stability boundary of the autopilot using the frequency method [10]. Frary [11] obtained a similar conclusion using a complete different method introduced by Garnell [10]. However, the pitch and yaw channels are separately treated during the autopilot design in all these previous investigations. Moreover, the analytical stability criterion of coning motion for spinning missiles with the attitude autopilot has not been given. As an extension of our previous study [1], this paper focuses on the stability of coning motion for spinning missiles with the attitude autopilot, and the stability boundary is analytically derived and demonstrated through mathematical simulations. Similar to our previous paper, the missile involved in this paper is also assumed to have tetragonal symmetry.

II. Structure of Attitude Autopilot for Spinning Missiles

A typical attitude autopilot mainly includes angular position feedback and angular velocity feedback. For a nonspinning missile, its airframe does not rotate continuously. Both the inertia sensors and the servo work in the same reference coordinate system (body coordinate system). Therefore, there is no need to consider the coordinate transformation between the feedback information and the command when analyzing the autopilot. The desired gain can be obtained by the conventional root locus or frequency approaches. But when a missile is spinning periodically, it is the nonspinning body coordinate that is considered as the reference coordinates of the autopilot, while it is still the body coordinate system for the servo. Therefore, the command transformation between the autopilot and servo must be taken into account.

For the short-period process of horizontal flight, the variation of attitude angle can be considered to be equivalent to that of the attack angle [1]. Therefore, the structure of the autopilot for a spinning missile can be established as shown in Fig. 1.

III. Mathematical Model of Closed-Loop System for Spinning Missile

A. Dynamic Model of Servo for Spinning Missile

Because of the spinning of missiles, there exist harmonic responses in the rudder angles under the constant commands. Given

Received 18 July 2010; revision received 25 August 2010; accepted for publication 26 August 2010.

*Ph.D. Student, School of Aerospace Engineering; yanyanbit@bit.edu.cn.
†Professor, School of Aerospace Engineering; yangshx@bit.edu.cn (Corresponding Author).
‡Postdoctoral Fellow, School of Aerospace Engineering; fenfenx@bit.edu.cn.

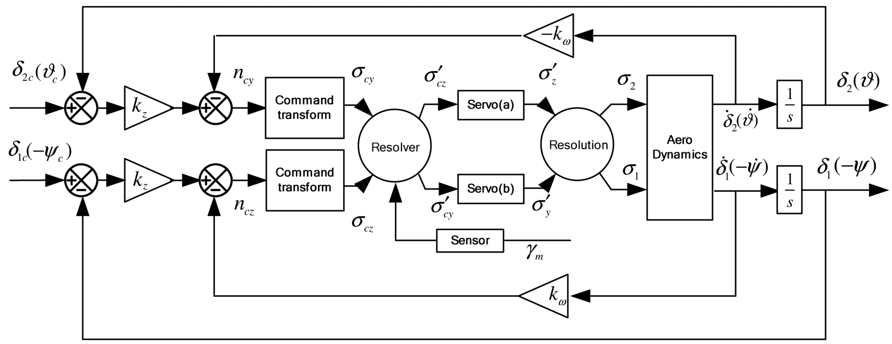

Fig. 1 Structure of autopilot for a spinning missile.

that the servo system can be modeled by a second-order system with natural frequency $1/T_s$ and damping ratio μ_s, and the command transmission delay τ is also considered, the relationship between the inputs and outputs of the servo in the nonspinning body coordinate for the spinning missiles can be obtained from [1]:

$$\begin{bmatrix} \sigma_1 \\ \sigma_2 \end{bmatrix} = k_s k_r \begin{bmatrix} \cos(\gamma_c + \tau\dot{\gamma}) & -\sin(\gamma_c + \tau\dot{\gamma}) \\ \sin(\gamma_c + \tau\dot{\gamma}) & \cos(\gamma_c + \tau\dot{\gamma}) \end{bmatrix} \begin{bmatrix} \sigma_{cy} \\ \sigma_{cz} \end{bmatrix} \quad (1)$$

where $\begin{bmatrix} \sigma_{cy} \\ \sigma_{cz} \end{bmatrix}$ and $\begin{bmatrix} \sigma_1 \\ \sigma_2 \end{bmatrix}$ are the commands and the response of rudder angles in the nonspinning body coordinate, respectively, k_s is the gain of the servo, $\gamma_c = \arccos \frac{1-T_s^2\dot{\gamma}^2}{\sqrt{(1-T_s^2\dot{\gamma}^2)^2+(2\mu_s T_s \dot{\gamma})^2}}$ is the steady-state deviation angle caused by the delay of servo dynamics and $k_r = \frac{1}{\sqrt{(1-T_s^2\dot{\gamma}^2)^2+(2\mu_s T_s \dot{\gamma})^2}}$ is the dynamic gain of the servo caused by the spinning of the missile.

B. Dynamics Model of Spinning Missiles

The spinning missiles not only have the common dynamic characteristics of nonspinning missiles with static stable moment and damping moment, but also have the Magnus and gyroscopic effects. We denote the nutation angle as δ, and its projection on the longitudinal and lateral planes as δ_2 and δ_1 respectively (see Fig. 2).

With the input of rudder angles, the governing equations of the dynamics of spinning missiles with tetragonal symmetry in terms of δ_2 and δ_1 can be obtained from [1]:

$$A\begin{bmatrix} \dot{\delta}_2 \\ \dot{\delta}_1 \end{bmatrix} + C\begin{bmatrix} -\ddot{\delta}_1 \\ \ddot{\delta}_2 \end{bmatrix} = \begin{bmatrix} -C_\delta \delta_1 - C_{\dot{\delta}}\dot{\delta}_1 - C_{\mathrm{ma}}\dot{\gamma}\delta_2 - C_r\sigma_1 \\ C_\delta \delta_2 + C_{\dot{\delta}}\dot{\delta}_2 - C_{\mathrm{ma}}\dot{\gamma}\delta_1 + C_r\sigma_2 \end{bmatrix} \quad (2)$$

Equation (2) describes the motion for spinning missiles with the presence of control moments, Magnus effects and gyroscopic effects induced by the spinning of the airframe.

C. Command Generation of Attitude Autopilots for Spinning Missiles

From Fig. 1, the command in the nonspinning body coordinate, denoted as n_{cy} and n_{cz}, can be obtained and represented as

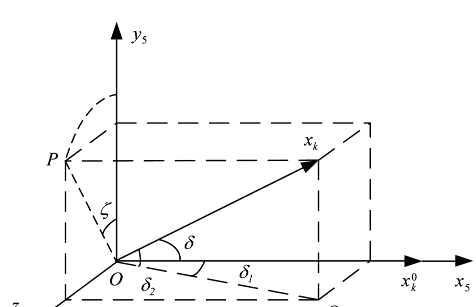

Fig. 2 Angle definitions relative to the velocity of missile.

$$\begin{bmatrix} n_{cz} \\ n_{cy} \end{bmatrix} = \begin{bmatrix} -k_\omega & 0 \\ 0 & -k_\omega \end{bmatrix} \begin{bmatrix} -\dot{\psi} \\ \dot{\vartheta} \end{bmatrix} + \begin{bmatrix} -k_z & 0 \\ 0 & -k_z \end{bmatrix} \begin{bmatrix} \delta_{1c} + \psi \\ \delta_{2c} - \vartheta \end{bmatrix} \quad (3)$$

It can be obtained from [1] that there exist both

$$\begin{cases} \dot{\delta}_1 = -\dot{\psi} \\ \dot{\delta}_2 = \dot{\vartheta} \end{cases} \quad \text{and} \quad \begin{cases} \delta_1 = -\psi \\ \delta_2 = \vartheta \end{cases}$$

Here we define that the negative-going deflection angle σ_{cy} produces positive-going maneuvering n_{cz}, and vice versa. Therefore, the control command of the servo in the nonspinning body coordinate is

$$\begin{bmatrix} \sigma_{cy} \\ \sigma_{cz} \end{bmatrix} = \begin{bmatrix} k_\omega \dot{\delta}_1 + k_z \delta_1 - k_z \delta_{1c} \\ -k_\omega \dot{\delta}_2 - k_z \delta_2 + k_z \delta_{2c} \end{bmatrix} \quad (4)$$

Denoting the deviation angle of servo system under spinning $(\gamma_c + \tau\dot{\gamma})$ as γ_d, one can obtain the actual output equation of the servo by substituting Eq. (4) into Eq. (1):

$$\begin{bmatrix} \sigma_1 \\ \sigma_2 \end{bmatrix} = k_r k_s \begin{bmatrix} \cos\gamma_d & -\sin\gamma_d \\ \sin\gamma_d & \cos\gamma_d \end{bmatrix} \begin{bmatrix} -k_\omega \dot{\delta}_1 - k_z \delta_1 + k_z \delta_{1c} \\ -k_\omega \dot{\delta}_2 - k_z \delta_2 + k_z \delta_{2c} \end{bmatrix} \quad (5)$$

Without the loss of generality, the input control commands δ_{1c} and δ_{2c} are both assumed as zero in the stability analysis. The deflection angle is defined in the form of complex number ($\sigma = \sigma_1 + i\sigma_2$), then Eq. (5) can be expressed as

$$\sigma = -k_r k_s k_\omega (\cos\gamma_d - i\sin\gamma_d)\dot{\delta} - k_r k_s k_z (\cos\gamma_d - i\sin\gamma_d)\delta \quad (6)$$

Equation (6) describes the projection of the real deflection angle in the nonspinning body coordinate for a spinning missile with an attitude autopilot from the complex domain point of view. The imaginary part indicates the existence of cross-coupling effects. It is found that the magnitude of the actual deviation of the servo response rises at increasing γ_d.

IV. Stability of Spinning Missiles with Attitude Autopilots

A. Stability Boundary of Spinning Missiles with Attitude Autopilots

When considering the stability of missiles with attitude autopilots, the distribution of the characteristic roots of the closed-loop system should be considered. To facilitate the analysis, the nutation angle is defined, in the complex form as $\delta = \delta_1 + i\delta_2$. After substituting $\delta = \delta_1 + i\delta_2$ into Eq. (2), the closed-loop system equation can be expressed as

$$C\ddot{\delta} + iA\dot{\delta} - C_{\dot{\delta}}\dot{\delta} - C_\delta \delta + iC_{\mathrm{ma}}\dot{\gamma}\delta - C_r\sigma = 0 \quad (7)$$

Substituting Eq. (6) into Eq. (7) yields

$$C\ddot{\delta} + [iA - C_{\dot{\delta}} + C_r k_r k_s k_\omega (\cos\gamma_d - i\sin\gamma_d)]\dot{\delta} + [-C_\delta + iC_{\mathrm{ma}}\dot{\gamma} + C_r k_r k_s k_z (\cos\gamma_d - i\sin\gamma_d)]\delta = 0 \quad (8)$$

Equation (8) can be further simplified as

$$C\ddot{\delta} - B\dot{\delta} + D\delta = 0 \tag{9}$$

where $B = (C_{\dot{\delta}} - C_r k_r k_s k_\omega \cos\gamma_d) + i(C_r k_r k_s k_\omega \sin\gamma_d - A)$:

$$D = (C_r k_r k_s k_z \cos\gamma_d - C_\delta) + i(C_{\text{ma}}\dot{\gamma} - C_r k_r k_s k_z \sin\gamma_d)$$

Denoting the real part and imaginary part of B as B_{Re} and B_{Im} respectively, to reach

$$B = B_{\text{Re}} + B_{\text{Im}} i \tag{10}$$

where $B_{\text{Re}} = C_{\dot{\delta}} - C_r k_r k_s k_\omega \cos\gamma_d$, $B_{\text{Im}} = C_r k_r k_s k_\omega \sin\gamma_d - A$.

Assuming $B^2 - 4CD = P + Qi$, one can derive the expression of P and Q as

$$\begin{cases} P = (C_r k_r k_s k_\omega \cos\gamma_d - C_{\dot{\delta}})^2 - (C_r k_r k_s k_\omega \sin\gamma_d - A)^2 \\ \quad - 4C(C_r k_r k_s k_z \cos\gamma_d - C_\delta) \\ Q = 2(C_{\dot{\delta}} - C_r k_r k_s k_\omega \cos\gamma_d)(A - C_r k_r k_s k_\omega \sin\gamma_d) \\ \quad - 4C(C_{\text{ma}}\dot{\gamma} - C_r k_r k_s k_z \sin\gamma_d) \end{cases} \tag{11}$$

The characteristic roots of Eq. (9) are given by

$$\lambda_{1,2} = \frac{B_{\text{Re}} + B_{\text{Im}} i \pm \sqrt{P + Qi}}{2C} \tag{12}$$

Defining $R = \sqrt{P^2 + Q^2}$, the characteristic roots in Eq. (12) can be rewritten as

$$\lambda_{1,2} = \frac{1}{2C}\left(B_{\text{Re}} \pm \sqrt{\frac{R+P}{2}}\right) + \frac{1}{2C}\left(B_{\text{Im}} \pm \sqrt{\frac{R-P}{2}}\right) i \tag{13}$$

Basically, since the stability of the system depends on the real part of the system characteristic root, our analysis focuses on the real part of the root. Evidently, the real parts $\lambda_{R(1,2)}$ of the characteristic roots $\lambda_{1,2}$ can be rewritten as below after substituting the expression of B_{Re} into Eq. (13):

$$\lambda_{R(1,2)} = \left(C_{\dot{\delta}} - k_r k_s k_\omega C_r \cos\gamma_d \pm \sqrt{\frac{R+P}{2}}\right) / 2C \tag{14}$$

Evidently, the coning motion for δ converges only if $\lambda_{R(1,2)}$ are negative, i.e.,

$$C_{\dot{\delta}} - k_r k_s k_\omega C_r \cos\gamma_d \pm \sqrt{\frac{R+P}{2}} < 0 \tag{15}$$

Since $\sqrt{\frac{R+P}{2}} \geq 0$, Eq. (15) holds true only when

$$C_{\dot{\delta}} - k_r k_s k_\omega C_r \cos\gamma_d < 0 \tag{16}$$

Meanwhile one should have

$$(C_{\dot{\delta}} - k_r k_s k_\omega C_r \cos\gamma_d)^2 > \frac{R+P}{2} \tag{17}$$

Substituting P and Q into the right part of inequality (17) yields

$$\begin{aligned} &(C_{\dot{\delta}} - k_r k_s k_\omega C_r \cos\gamma_d)^2 (C_r k_r k_s k_z \cos\gamma_d - C_\delta) > \\ &\quad C(C_{\text{ma}}\dot{\gamma} - C_r k_r k_s k_z \sin\gamma_d)^2 - (C_{\dot{\delta}} - C_r k_r k_s k_\omega \cos\gamma_d) \\ &\quad \times (A - C_r k_r k_s k_\omega \sin\gamma_d)(C_{\text{ma}}\dot{\gamma} - C_r k_r k_s k_z \sin\gamma_d) \end{aligned} \tag{18}$$

By combining inequalities (16) and (17), the stability condition of spinning missiles with attitude autopilots is finally obtained:

$$\begin{cases} C_{\dot{\delta}} - k_r k_s k_\omega C_r \cos\gamma_d < 0 \\ (C_{\dot{\delta}} - k_r k_s k_\omega C_r \cos\gamma_d)^2 (C_r k_r k_s k_z \cos\gamma_d - C_\delta) > \end{cases} \tag{19a}$$

$$\begin{cases} C(C_{\text{ma}}\dot{\gamma} - C_r k_r k_s k_z \sin\gamma_d)^2 \\ -(C_{\dot{\delta}} - C_r k_r k_s k_\omega \cos\gamma_d)(A - C_r k_r k_s k_\omega \sin\gamma_d) \\ (C_{\text{ma}}\dot{\gamma} - C_r k_r k_s k_z \sin\gamma_d) \end{cases} \tag{19b}$$

Inequality (19) is the necessary and sufficient condition for the coning motion to converge. Both the damping-loop gain and the forward gain should meet both parts of inequality (19).

B. Discussion of the Stability Condition

From inequality (19a), when $\gamma_d > 90°$, the upper limit of the damping-loop gain is restrained:

$$k_\omega < \frac{C_{\dot{\delta}}}{k_r k_s C_r \cos\gamma_d} \tag{20}$$

$C_{\dot{\delta}}$ is generally very small because of the weak damping characteristic of missiles. When the total delay angle γ_d is larger than 90°, a larger damping-loop gain k_ω will destabilize the system. This conclusion is consistent to the results in [1]. Inequality (19b) exerts another restriction on the damping-loop gain and the attitude-loop gain.

To further explain the variations of the limit boundary of the attitude autopilot when the missile is spinning, some simplification is adopted to show the impact on the system stability when the control system is introduced. By assuming $\gamma_d < 90°$ and neglecting the Magnus and gyro effects, the stability condition (19) can be simplified as

$$\begin{aligned} &(k_r k_s k_\omega C_r \cos\gamma_d)^2 (C_r k_r k_s k_z \cos\gamma_d - C_\delta) > C(C_r k_r k_s k_z \sin\gamma_d)^2 \\ &\quad + (C_r k_r k_s k_\omega \cos\gamma_d)(C_r k_r k_s k_\omega \sin\gamma_d)(C_r k_r k_s k_z \sin\gamma_d) \end{aligned} \tag{21}$$

Let $K_\omega = k_r k_s k_\omega C_r$ and $K_z = k_r k_s k_z C_r$, inequality (21) can be simplified as

$$K_\omega^2[\cos^2\gamma_d(K_z\cos\gamma_d - C_\delta) - K_z\sin^2\gamma_d\cos\gamma_d] > CK_z^2\sin^2\gamma_d \tag{22}$$

It is clear that the prerequisite to ensure inequality (22) is

$$\cos^2\gamma_d(K_z\cos\gamma_d - C_\delta) - K_z\sin^2\gamma_d\cos\gamma_d > 0 \tag{23}$$

After simplification, inequality (23) can be rewritten as

$$K_z\left(\cos\gamma_d - \frac{\sin^2\gamma_d}{\cos\gamma_d}\right) > C_\delta \tag{24}$$

Inequality (24) indicates that γ_d induces an additional restriction on K_z and clearly the value of γ_d has significant impact on the sign of inequality (24). Detailed discussion with respect to the value of γ_d is presented below.

1) When $\gamma_d \leq 45°$, the left hand side of inequality (24) is nonnegative. Inequality (24) is definitely true because $C_\delta < 0$ holds for static stable missiles. Inequality (22) can be rewritten as

$$K_\omega > \sqrt{\frac{C\sin^2\gamma_d K_z^2}{\cos^2\gamma_d(K_z\cos\gamma_d - C_\delta) - K_z\sin^2\gamma_d\cos\gamma_d}} \tag{25}$$

Inequality (25) represents the stability boundary when the coning motion of missiles with an attitude autopilot is convergent under the situation $\gamma_d \leq 45°$. It means that k_ω impacts the upper bound of k_z due to γ_d. The physical interpretation is that the cross-coupling of servo is related to the gain k_z when the attitude feedback works. When k_z is larger, the cross-coupling effect will lower the system stability margin. However, if larger damping exists, the system can be still stable. Otherwise, the system is unstable owing to the instability of coning motion. The relationship between the values of the design parameters for autopilot (k_z and k_ω) and the system stability boundary is illustrated in Fig. 3. The bottom right area of the stability boundary (shadow area) represents the region where the stability condition is possibly not satisfied. From Fig. 3, it is noticed that the stable region decreases remarkably as γ_d increases. It means that only

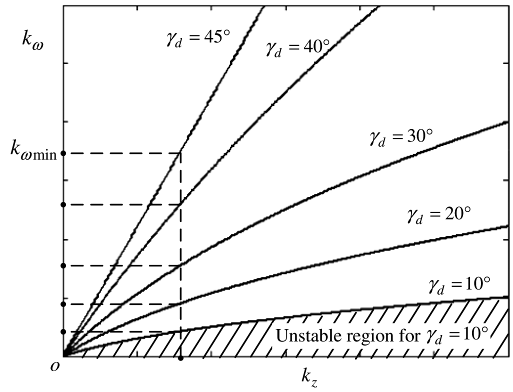

Fig. 3 Illustration of the stable region for different gains.

a smaller k_z can be selected at larger k_ω and γ_d, corresponding to a lower response servo system.

From Fig. 3, it is found that with the increase of the delay angle γ_d, the system stable region is shrinking, and the requirement on the damping is increasing for a given k_z. Evidently, to design an autopilot for a spinning missile with prespecified performance, it is crucial to choose a proper k_z according to the autopilot bandwidth requirement and choose a better k_ω to improve the dynamic response while inequality (25) is satisfied.

2) When $45° < \gamma_d < 90°$, both sides of inequality (24) are negative. Inequality (24) can be rewritten as

$$K_z < \frac{\cos\gamma_d}{\cos 2\gamma_d} C_\delta \tag{26}$$

To ensure the conning motion convergence, the stability boundary is represented in two inequalities (25) and (26). An additional restriction on the selection of K_z appears. K_z can only be selected from 0 to $-C_\delta$ depending on γ_d when $\gamma_d > 60°$. Because the absolute value of C_δ is small, K_z must be small. Clearly, the loop gain denoted by $-K_z/C_\delta$ is also small. It is difficult to design a satisfactory attitude autopilot with a small loop gain, and there is no way to design an attitude autopilot under the extreme condition in which the autopilot almost degenerates to a rate loop. Therefore, it is a great challenge to design an autopilot with satisfactory performances when a lower response servo system is used.

C. Method to Increase the Stability Limits

From the derivation, it is noticed that it is the cross-coupling caused by the spinning that narrows the stability limits. This means that the decoupling methods, such as prerotating the commands to the servo system can be used to correct the total delay angle and increase the stability limits. This can be achieved by setting a lead angle γ_l for the commands according to the total delay angle γ_d. The actual total delay angle will be reduced to zero at a constant spinning rate when $\gamma_l = -\gamma_d$. In this case, the inequalities (25) and (26) will hold true because $\gamma_d = 0$, and therefore the stability limits will be greatly increased. In the case when the spinning rate varies, the lead angle can be selected according to γ_d at the average spinning rate. The actual total delay angle can also be significantly decreased with this method, thus the stability limits could be increased, although the total delay angle can not be compensated completely. It is convenient to apply this method to engineering problems and the benefits will be illustrated in the following section.

V. Simulation Verification

To demonstrate the proposed method, a case study of a spinning missile is conducted. The parameters of the spinning missile are listed in Table 1.

First the stability limit gain k_z (denoted as k_{z0}) corresponding to different damping-loop gain k_ω is calculated using the conventional root locus design method [10]. Then another stability limit gain k_z (denoted as k'_{z0}) is also obtained by our method proposed in this paper. The results are shown in Table 2.

From Table 2, it is noted that the stability limit of the attitude-loop gain is significantly reduced due to the spinning of the missile. The results obtained by the conventional method may even exceed the stability boundary for spinning missiles obtained with the present method. For example, when $k_\omega = 0.4$, the critical k_z is 12.78 by the conventional method, while it is reduced to 0.7771 for the spinning missile ($\dot{\gamma} = 10\pi$ rad/s).

Simulation of the nonlinear model, which takes all the nonlinear terms approximated during the derivation of Eq. (2) such as $\frac{\sin\delta_1}{\sin\delta_2}\cos\delta_2 \approx \frac{\delta_1}{\delta_2}$, $\arcsin(\sqrt{\sin^2\delta_2 + \cos^2\delta_2\sin^2\delta_1}) \approx \sqrt{\delta_1^2 + \delta_2^2}$ and the neglect of high-order terms, etc., into account, is also conducted to verify the stability limit obtained by our proposed method. When the damping-loop gain $k_\omega = 0.6$, the attitude-loop adjust gain $k_z = 13$ and the spinning rate is $\dot{\gamma} = 10\pi$ rad/s, the system is considered as stable according to the conventional method, but unstable with our proposed approach. As illustrated in Fig. 4, the attitude angle is clearly divergent. From Fig. 4b, we see that the conning motion is divergent with right-handed rotation when viewed from the tail.

At attitude-loop gain $k_z = 0.8725$, which is the critical value by our method, the simulation results are shown in Fig. 5. It is observed that for this critical state, the attitude angle of the missile shows periodic oscillation with constant amplitude, and the missile is in the limit cycle state.

At $k_z = 0.4$, which satisfies the stability requirement, the simulation results are illustrated in Fig. 6. The initial disturbance decays and the conning motion approaches to the zero point with the right-handed rotation.

Evidently, the stability limit of the coning motion for a spinning missile derived by our approach shows a great agreement to the simulation results.

To demonstrate the effectiveness of the decoupling approach of setting a lead angle for the commands to the servo system, the stability limit gain k_z obtained at different constant and varying spinning rates for the same k_ω and k_{z0} in Table 2 is displayed in Table 3.

It is noted that compared with the counterparts in Table 2, k'_{z0} corresponding to $\dot{\gamma} = 8\pi$ rad/s and $\dot{\gamma} = 12\pi$ rad/s in Table 3 is greatly increased with the employment of the decoupling method. When $\dot{\gamma} = 8\pi$ rad/s, the stability limits with compensation (k'_{z0}) are even greater than those obtained by the conventional method (k_{z0}). The reason is that γ_l compensates not only the phase lag of the servo system but also the command transmission delay τ. It is also observed that k'_{z0} at $\dot{\gamma} = 12\pi$ rad/s is smaller than that at $\dot{\gamma} = 8\pi$ rad/s. The interpretation lies in that within the decoupling method only the phase lag is taken into account, while the amplitude is out of consideration. Remarkable increase in the stability limits is also observed with varying spinning rates (see the fifth column of Table 3) comparing to those in Table 2 (see the fifth column of Table 2), although they are still smaller than k_{z0}. Evidently, this decoupling

Table 1 Parameters of a spinning missile

Parameter	Value	Parameter	Value
C_δ	-0.6522	$A/\dot{\gamma}$	1.4×10^{-4}
$C_{\dot{\delta}}$	-8.275×10^{-3}	C	0.0319
C_r	5.458×10^{-2}	T_s	0.016
C_{ma}	-2.1725×10^{-4}	μ_s	0.5
k_s	10	τ, ms	15

Table 2 Stability limit at different spinning rates

k_ω	k_{z0}	k'_{z0}		
		$\dot{\gamma} = 8\pi$ rad/s	$\dot{\gamma} = 10\pi$ rad/s	$\dot{\gamma} = 12\pi$ rad/s
0.2	6.32	1.3269	0.5533	0.2026
0.4	12.78	2.4632	0.7771	0.2559
0.5	15.3	2.9782	0.8341	0.2668
0.6	18.3	3.4491	0.8725	0.2734
0.8	23.1	4.2869	0.9184	0.2808

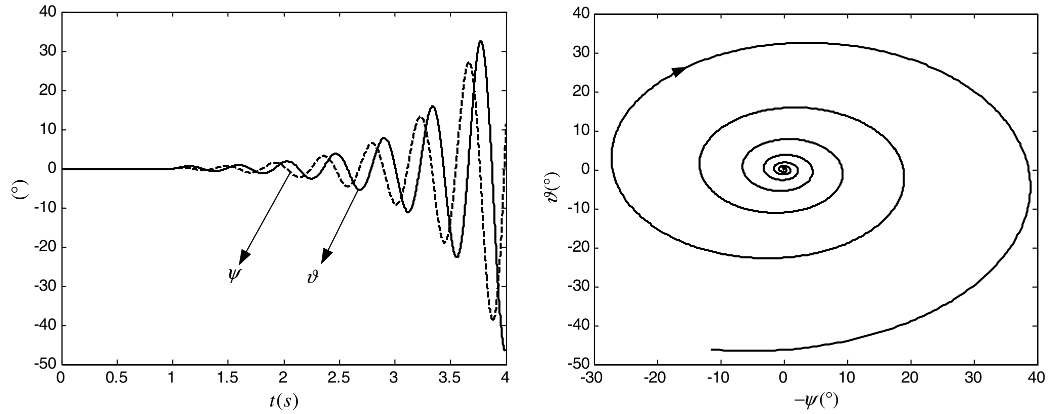

a) Curve of attitude angle
b) Unstable conning motion

Fig. 4 Simulation results for $k_\omega = 0.6, k_z = 13$.

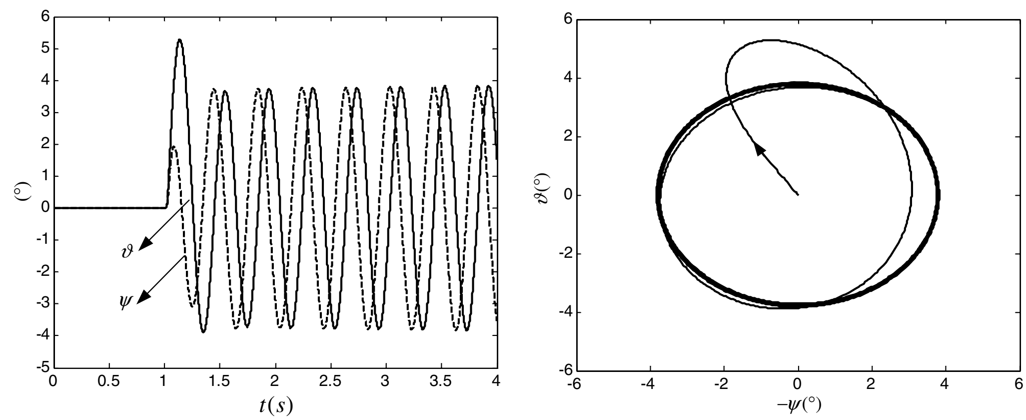

a) Curve of attitude angle
b) The critical conning motion

Fig. 5 Simulation results for critical state for $k_\omega = 0.6, k_z = 0.8725$.

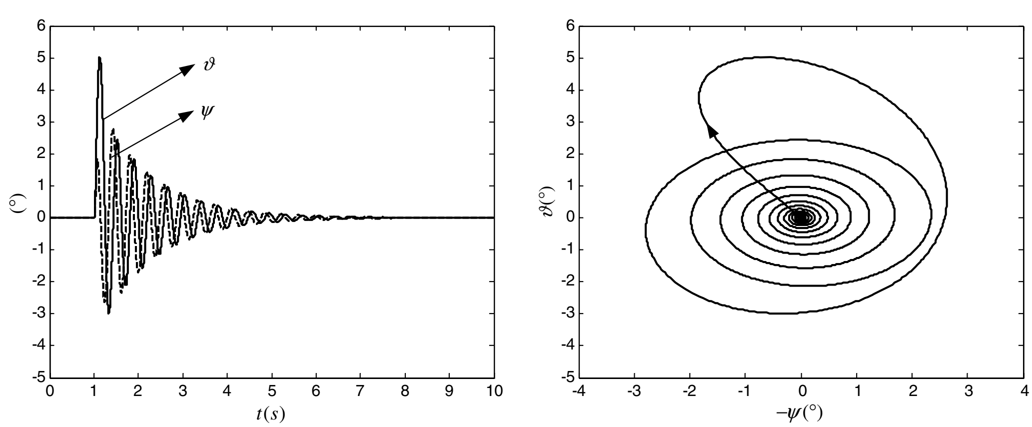

a) Curve of attitude angle
b) The stable conning motion

Fig. 6 Simulation results for $k_\omega = 0.6, k_z = 0.4$.

Table 3 Stability limit with lead angle at different spinning rates

k_ω	k_{z0}	k'_{z0}		
		$\dot{\gamma} = 8\pi$ rad/s $\gamma_l = 0.82$ rad	$\dot{\gamma} = 12\pi$ rad/s $\gamma_l = 1.32$ rad	$\dot{\gamma} = 8\pi \sim 12\pi$ rad/s $\gamma_l = 1.06$ rad
0.2	6.32	8.19	7.31	3.28
0.4	12.78	15.31	12.82	6.64
0.5	15.3	19.17	15.31	8.43
0.6	18.3	21.84	17.81	10.21
0.8	23.1	27.64	22.32	13.52

method can greatly increase the stability limits in cases with constant and varying spinning rates.

VI. Conclusions

In this paper, the sufficient and necessary condition of the coning motion stability of spinning missiles with attitude autopilots is analytically derived and further verified by the mathematical simulation on the nonlinear model. It is noticed that the stable region of the design parameters for the attitude autopilot shrinks so significantly due to the spinning of the missile that it is almost impossible to ensure the stability of an autopilot by means of the conventional method. In the design of an autopilot, it is required to check the applicability of the design parameters according to the stability boundary when the missile is subjected to spinning. Analysis results from the stability condition indicate that the spinning missile must employ servo system with faster response to lower the total delay angle. And only when the total delay angle is smaller than 45°, can the desired attitude autopilot be designed. From the derivation, it is also noticed that it is the cross-coupling caused by the spinning that narrows the stability limits. This result implies that the decoupling methods, such as prerotating the commands in the opposite direction, the dynamic inverse theory, etc., can be used to correct the total delay angle and increase the stability limits. The stability boundary criteria given in this paper can be applied to the engineering design of attitude autopilots for spinning missiles.

Acknowledgment

The grant support from National Science Foundation of China (No. 10972034) is greatly acknowledged.

References

[1] Yan, X., Yang, S., and Zhang, C., "Coning Motion of Spinning Missiles Induced by the Rate Loop," *Journal of Guidance, Control, and Dynamics*, Vol. 33, No. 5, 2010, pp. 1490–1499. doi:10.2514/1.48041

[2] Mao, X., Yang, S., and Xu, Y., "Coning Motion Stability of Wrap Around Fin Rockets," *Science in China Series E, Technological Sciences*, Vol. 50, No. 3, 2007, pp. 343–350. doi:10.1007/s11431-007-0026-0

[3] Linao, G., and Morote, J., "Roll-Rate Stability Limits of Unguided Rockets with Wraparound Fins," *Journal of Spacecraft and Rockets*, Vol. 43, No. 4, 2006, pp. 757–761. doi:10.2514/1.17775

[4] Morote, J., and Linao, G., "Flight Dynamics of Unguided Rockets with Free-Rolling Wrap Around Tail Fins," *Journal of Spacecraft and Rockets*, Vol. 43, No. 6, 2006, pp. 1422–1423. doi:10.2514/1.22645

[5] Mracek, C. P., Stafford, M., and Unger, M., "Control of Spinning Symmetric Airframes," National Technical Information Service Rept. ADA466818, Nov. 2006.

[6] Zipfel, P. H., *Modeling and Simulation of Aerospace Vehicle Dynamics*, 2nd ed., AIAA, Reston, VA, 2007.

[7] Creagh, M. A., and Mee, D. J., "Attitude Guidance for Spinning Vehicle with Independent Pitch and Yaw Control," *Journal of Guidance, Control, and Dynamics*, Vol. 33, No. 3, 2010, pp. 915–922. doi:10.2514/1.44430

[8] Elias, R., "Active Nutation and Precession Control for Exoatmospheric Spinning Ballistic Missiles," AIAA Paper 2008-6998, Aug. 2008.

[9] Lestage. R., "Analysis of Control and Guidance of Rolling Missiles with a Single Plane of Control Fins," AIAA Paper 2000-3971, Aug. 2000.

[10] Garnell, P., *Guided Weapon Control Systems*, 2nd ed., Pergamon, New York, 1980. pp. 118–126.

[11] Frary, D. J., "The Prediction of Autopilot Behavior in the Presence of Roll Motion," British Aircraft Co., Rept. ST5686, May 1971.